Theor Chem Acc (2012) 131:1210
DOI 10.1007/s00214-012-1210-2

REGULAR ARTICLE

Theoretical simulations of the vibrational predissociation spectra of H_5^+ and D_5^+ clusters

Alvaro Valdés · Patricia Barragán · Cristina Sanz-Sanz · Rita Prosmiti · Pablo Villarreal · Gerardo Delgado-Barrio

Received: 7 February 2012 / Accepted: 20 March 2012 / Published online: 7 April 2012

Abstract In the present study, the effect of the potential energy surface representation on the infrared spectra features of the H_5^+ and D_5^+ clusters is investigated. For the spectral simulations, we adopted a recently proposed (Sanz-Sanz et al. in Phys Rev A 84:060502-1–4, 2011) two-dimensional adiabatic quantum model to describe the proton-transfer motion between the two H_2 or D_2 units. The reported calculations make use of a reliable "on the fly" DFT-based potential surface and the corresponding new dipole moment surface. The results of the vibrational predissociation dynamics are compared with earlier and recent experimental data available from mass-selected photodissociation spectroscopy, as well as with previous theoretical calculations based on an analytical ab initio parameterized surfaces. The role of the potential topology on the spectral features is studied, and general trends are discussed.

Keywords Potential energy surfaces · Electronic structure calculations · Spectrum simulations

Dedicated to Professor Marco Antonio Chaer Nascimento and published as part of the special collection of articles celebrating his 65th birthday.

A. Valdés · C. Sanz-Sanz · R. Prosmiti (✉) · P. Villarreal · G. Delgado-Barrio
Instituto de Física Fundamental, C.S.I.C.,
Serrano 123, 28006 Madrid, Spain
e-mail: rita@iff.csic.es

P. Barragán
CELIA, Université de Bordeaux-I, UMR CNRS 5107, CEA,
351 Cours de la Libération, 33045 Talence, France

C. Sanz-Sanz · R. Prosmiti · P. Villarreal · G. Delgado-Barrio
Unidad Asociada, UAM-CSIC, Departamento de Química Física, Facultad de Ciencias C-XIV,
Universidad Autónoma de Madrid, 28049 Madrid, Spain

1 Introduction

H_5^+ has been first detected in 1962 [1], and since then several experimental studies have been carried out, although the information available is rather limited to dissociation enthalpies [2–4] and a few vibrational frequencies at energies between 2,500 and 8,000 cm^{-1} [5–7]. Directly related to this work are the experiments reported by Okumura et al. [5] in 1988, later on by Bae [6], and just recently by Duncan et al. [7] on the infrared (IR) photodissociation spectra of the H_5^+. In the earlier investigations, three broad bands have been observed near 4, 000 cm^{-1} and have been assigned to vibrational frequencies of H_5^+, such as fundamental stretching modes of H_3^+ and H_2, as well as combinations or overtones of these modes with the intermolecular $H_3^+ + H_2$ [5]. However, in the latter study the excitation of the shared-proton stretch mode have been found to play a major role in the assignment of the same spectral features [7]. In particular, Duncan et al., in addition to the H_5^+ spectrum in the 2,000–4,500 cm^{-1}, have also recorded for the first time the D_5^+ one in the spectral region of 1,500–3,500 cm^{-1}. They showed that the delocalized and highly anharmonic shared-proton stretch mode carries very large oscillator strength, and its excitations are involved in the spectral transitions at the energy region studied [7]. Just recently, the importance of the proton-transfer stretching in the IR spectra of these clusters has been studied by applying an adiabatic two-dimensional model incorporating the temperature effect [8].

However, despite the apparent simplicity and the effort devoted, very little is still known about the spectroscopic

characterization even at low vibrational energies, and finite-temperature properties of H_5^+ and its isotopes [7, 9–12]. For theoretical studies, the main difficulty arises from the very delicate relationship between the interaction potential energy surface (PES) and experimental observations. Comparison of theoretical results with experimental data is subject to the errors coming from the poor, in general, knowledge of the PES, the dynamical approximations adopted, and the uncertainties of the experimental measurements. As the number of atoms increases, the route to accurate interaction PESs is hard, as it depends on the complexity of the system.

Until recently, there was not global potential energy surface available in the literature for the H_5^+, while numerous ab initio calculations at various levels of theory have been reported [13–21], although they were limited to local description of the PES. However, during the last years three surfaces have been reported in the literature claiming a full-dimensional and reliable description of the H_5^+ cluster [22–24]. Two of them have been generated from analytical expressions parameterized to high-level CCSD(T) ab initio data [22, 23], while the third one is obtained from "on the fly" DFT calculations [24].

Simplified models to perform spectra simulations, as the one proposed recently [8], allow to explore the effect of the underlying surface and to evaluate the role of the possible differences between several of them on the dynamics of the system. Therefore, in the present study, by analyzing spectral features, we are able to rationalize the trends within the spectra and relate them to the properties of the topology of the PES of both H_5^+ and D_5^+ complexes. For this purpose, we use the two more recent PESs that were obtained from completely different generation procedures [23, 24].

The plan of this paper is as follows. Section 2 describes the coordinate system and the representation of the Hamiltonian together with computational details for the spectra simulations. In Sect. 3, we present the results obtained and discuss their comparison with previous experimental and theoretical data, while Sect. 4 summarizes our conclusions.

2 Coordinate system, model Hamiltonian operator, and computational details

The coordinate system used for describing the H_5^+ and D_5^+ clusters is shown in Fig. 1. The positions of the centers of mass of the two H_2 monomers, together with the position of the proton, define the two z_1 and z_2 distances with the coordinates used to be defined as $r = z_1 - z_2$ and $R = z_1 + z_2$ with $0 \le R \le \infty$ and $-R \le r \le R$. The Hamiltonian operator is given as [8]:

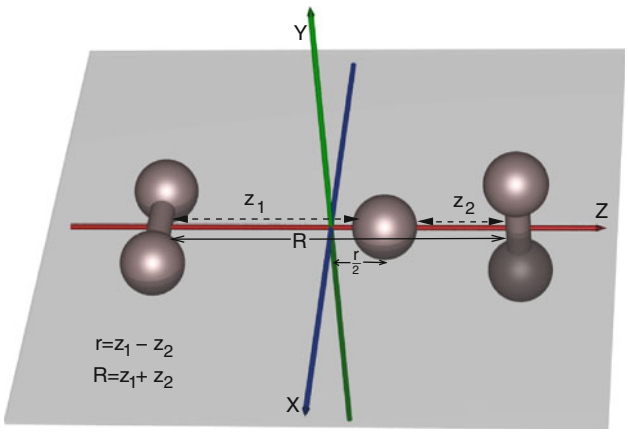

Fig. 1 2D Coordinate system used for the H_5^+ and D_5^+ complexes

$$\hat{H} = -\frac{\hbar^2}{2}\left(\frac{1}{\mu_r}\frac{\partial^2}{\partial r^2} + \frac{1}{\mu_R}\frac{\partial^2}{\partial R^2} + \frac{2}{\mu_{rR}}\frac{\partial^2}{\partial r \partial R}\right) + V(r,R) = T_r + T_R + T_{rR} + V(r,R), \quad (1)$$

with $V(r, R)$ the potential energy surface of the system. In our case, $\mu_r = m/5$, $\mu_R = m$ with m the hydrogen or deuterium mass. The reduced masses of the two H_2 or D_2 monomers, for example $\mu_{12} = \mu_{34} = \frac{m}{2}$, are the same, so the $\frac{1}{\mu_{rR}} = \frac{1}{\mu_{12}} - \frac{1}{\mu_{34}}$ is zero. Thus, the crossing kinetic term T_{rR} vanishes, and given the mass difference in the r and R coordinates, we can assume an adiabatic separation by approximating the total wavefunction as $\Phi(r,R) \approx \phi_v(r;R)\psi_{v\epsilon}(R)$. For a given v, the corresponding R-dependent eigenvalues, $W_v(R)$, computed from the

$$[T_r + V(r,R) - W_v(R)]\phi_v(r;R) = 0, \quad (2)$$

act as effective potentials in the Schrödinger equation,

$$[T_R + W_v(R) - \epsilon]\psi_{v\epsilon}(R) = 0. \quad (3)$$

to obtain discrete $(\epsilon < W_v(R \to \infty)$, $\epsilon = E_{vn}$, $n = 0, 1, \ldots)$ and continuum solutions $(\epsilon > W_v(R \to \infty))$ accounting for vibrations, n, in the R coordinate. The $\psi_{v'n'}$ vibrational excited states immersed in the continuum of $v'' < v'$ vibrational levels are coupled with the continuum wavefunctions, $\psi_{v''\epsilon}$, as follows:

$$\langle \Phi_{v''\epsilon}|\hat{H}|\Phi_{v'n'}\rangle = \langle \psi_{v''\epsilon}|Q_{v''v'}(R)|\psi_{v'n'}\rangle_R. \quad (4)$$

with the coupling operator $\hat{Q}$ being

$$\hat{Q} = 2\left\langle \phi_{v'}\left|\frac{\partial \phi_v}{\partial R}\right\rangle_r \frac{\partial}{\partial R} + \left\langle \phi_{v'}\left|\frac{\partial^2 \phi_v}{\partial R^2}\right\rangle_r \right. \right. = 2\frac{\langle \phi_{v'}|\frac{\partial V}{\partial R}|\phi_v\rangle}{W_v(R) - W_{v'}(R)}\frac{\partial}{\partial R} + \sum_{v'' \neq v' \neq v} \frac{\langle \phi_{v'}|\frac{\partial V}{\partial R}|\phi_{v''}\rangle\langle \phi_{v''}|\frac{\partial V}{\partial R}|\phi_v\rangle}{[W_{v''}(R) - W_{v'}(R)][W_v(R) - W_{v''}(R)]} \quad (5)$$

where the Hellmann–Feynman theorem has been used.

The process we pretend to simulate corresponds to the promotion of an initial vibrational state $|\Phi_{vn}\rangle$ to a intermediate or final $|\Phi_{v'n'}\rangle$ one of the H_5^+, as follows:

$$H_5^+(v,n) + \hbar\omega \rightarrow H_5^+(v',n') \rightarrow H_3^+ + H_2 + \epsilon \quad (6)$$

This excitation takes place within the same electronic state by the absorption of a photon with frequency, ω, that matches with the energy difference of these two vibrational states and is in the infrared spectral region:

By considering a Boltzmann distribution over the initial states at temperature T, the line intensity for such transitions is given by

$$I_{v'n',vn} \propto \frac{e^{-(E_{vn}/kT)}}{\sum_{v,n} e^{-(E_{vn}/kT)}} |\mu_{v'n';vn}|^2 \quad (7)$$

and would appear at a the photon frequency $\omega_{v'n',vn} = (E_{v'n'} - E_{vn})/\hbar$. The $\mu_{v'n',vn} = \langle \Phi_{v'n'}|\mu|\Phi_{vn}\rangle$ are the corresponding transition dipole moments, and $\mu(r, R)$ the dipole moment surface of the system. The absorption of a photon that leads to a vibrational excitation of the cluster may be followed by energy transfer to weaker bonds causing the dissociation of the cluster. This process is known as vibrational predissociation and it produces broadening of the corresponding spectral lines. In the Golden rule approximation [25], the half-width associated with the vibrational predissociation of an initial state $\psi_{v'n'}$ into a final continuum state $\psi_{v''\epsilon}$ is given by

$$\Gamma_{v'n'} = \pi \sum_{v''<v'} \left|\langle \psi_{v''\epsilon}|Q_{v''v'}(R)|\psi_{v'n'}\rangle_R\right|^2, \quad (8)$$

where the $\psi_{v''\epsilon}$ is calculated for an energy $\epsilon = E_{v'n'} - W_{v''}(R \rightarrow \infty)$, which corresponds, for large R distance, to the relative energy between the H_3^+ and H_2 fragments. Then, by dressing the corresponding lines in the spectrum with Lorentzian functions of $\Gamma_{v'n'}$ widths, and by summing over transitions [26], a continuum spectrum is obtained,

$$I(\omega) = \sum_{v'n'vn} \frac{\Gamma_{v'n'}/2\pi}{\hbar^2(\omega - \omega_{v'n',vn})^2 + \Gamma_{v'n'}^2/4} I_{v'n',vn} \quad (9)$$

which satisfies the condition $\int d\omega I(\omega) = \sum_{v'n'vn} I_{v'n',vn}$.

3 Results and discussion

As we mentioned above, up to date, there are three PESs available in the literature for the H_5^+, [22–24]; however, we consider here the two more recent ones. On the one hand, an analytical representation of the PES based on a TRIM (triatomics-in-molecules) formalism, which has been parameterized to high-level CCSD(T) data [23] and has been previously employed in spectral simulations [8, 27]. On the other hand, an "on the fly" surface based on DFT calculations [24] using a specific hybrid functional, B3(H), which has been specially designed for hydrogen-only systems [28]. As it can be seen, these two surfaces have been generated from completely different procedures, and thus several differences have been found between them. The main ones are the predictions of the D_e well-depth energy: the DFT surface overestimates it compared to the CCSD(T)/CBS results [21], and regarding the barrier height for the internal proton transfer, the TRIM fitted surface overestimates it, while the DFT one underestimates it, taken as reference data the ones from CCSD(T)-R12 calculations [17].

For the present calculations, we employ the DFT-based potential for the H_5^+ [24]. Such representation has been found to correctly describe the overall surface of the cluster [24] and has been used in previous studies [10, 11, 29, 30].

In Fig. 2 (top panel) we show the potential curves as a function of r for the indicated R values. The potential curves are obtained by optimizing at each (r, R) point the bond lengths of the two perpendicular H_2 monomers (see Fig. 1). One can see that the potential curves are symmetric in the r coordinate for small R values, and the proton is moving in a single potential well around the D_{2d} configuration of the H_5^+. As the R distance increases, a double-well potential corresponding to C_{2v} geometries appears. These symmetric wells are separated by a D_{2d} barrier, which gets higher for larger values of R. Also we display in Fig. 2 (middle panel) the $\partial V/\partial R$ derivatives of the potential. We should point out here that the derivatives of the DFT potential show a very smooth behavior; they are symmetric and thus only allow states of the same symmetry (even or odd) to be coupled by the kinetic coupling terms $Q_{v''v'}$ in Eq. 5.

For the spectral calculations, the electric dipole moment surface is also needed, and we compute such surface here by performing DFT/B3(H) calculations, the same ones as for the potential. In Fig. 2 (bottom panel), we present the dipole moment curves as a function of r and R. One can see that for each R the dipole moment does not behave linearly for the whole range of r, although in the region of interest, values of r close to zero, is rather close to it. Also, it is an odd function leading to nonzero transition dipole moment, $\mu_{v'n',vn}$, for states of different symmetry.

In turn, by solving the Eqs. 2 and 3, we obtained the effective $W_v(R)$ potentials together with the corresponding ϕ_v states, as well as the E_{vn} bound or ϵ continuum levels, and their $\psi_{v\epsilon}$ wavefunctions. In Figs. 3 and 4, we present the six lowest $W_v(R)$ potentials, with $v = 0$–5, and the bound E_{vn}, with $n = 0$–10, levels up to 8,000 cm^{-1} for the H_5^+ and D_5^+, respectively. The ϕ_v are symmetric and antisymmetric states, and as it can be seen in Figs. 3 and 4, are degenerate for R values larger than 4.5 and 5.0 bohr for the

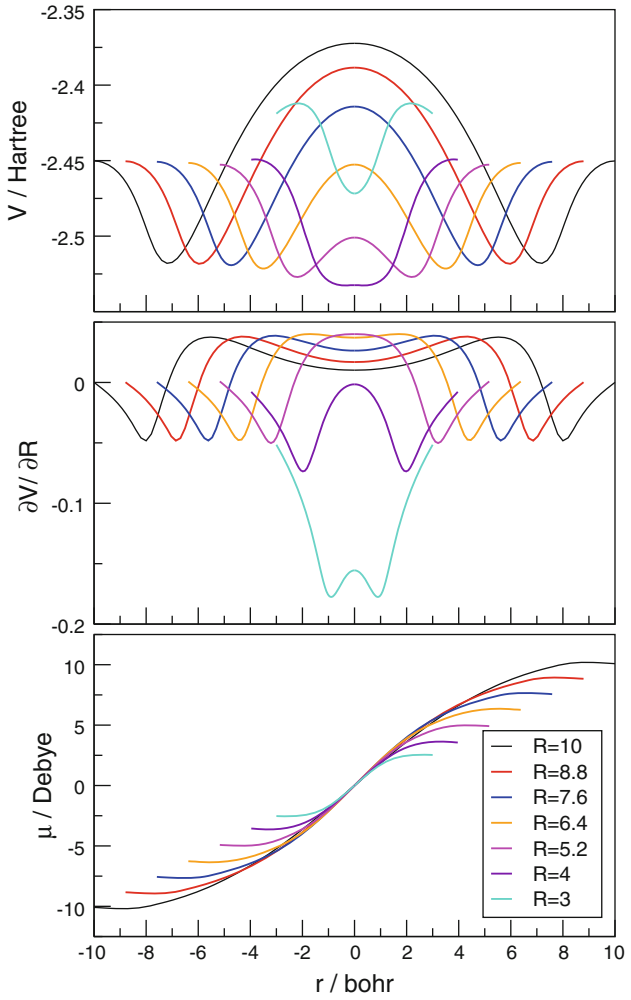

Fig. 2 Potential $V(r, R)$ curves (*top panel*), first derivatives with respect to R (*middle panel*), and the dipole moment $\mu(r, R)$ (*bottom panel*) for the H_5^+

H_5^+ and D_5^+, respectively. Based on the present 2D model, the dissociation energy, $D_0 = W_0(R \to \infty) - E_{00}$, is estimated to be 3,719 and 3,649 cm^{-1} for each ion. These values are overestimated compared with the full-dimensional ones of 2,455 ± 125 and 2,738 ± 206 cm^{-1} reported previously for the same DFT surface using path integral Monte Carlo (PIMC) [10, 11]. Therefore, we should note that for the H_5^+, the levels with $v < 2$ and the E_{20}, E_{21}, E_{30}, and E_{31} are discrete, while for the D_5^+, the levels show larger anharmonicity and more states, with $v = 0$ and 1 as well as the E_{20}, E_{21}, E_{23}, E_{30}, E_{31}, E_{32}, E_{40}, E_{41}, and E_{50} are actually discrete in this case.

The calculated IR continuum spectra, obtained from Eq. 9 using the DFT surface [24], over a large spectral range (up to 6,000 cm^{-1}) and at temperatures of 1 and 300 K (see top and bottom panels, respectively), are shown in Fig. 5 for the H_5^+ (left panels) and D_5^+ (right panels). For comparison reasons, in the same plot we also present the spectra obtained from the Ref. [8] with the analytical CCSD(T) parameterized surface [23], as well as (see inset plots) the experimental IR photodissociation spectra [7]. One can see that for the H_5^+ both calculated spectra at $T = 1$ K show the same spectral bands, with the energy position of the peaks to be blue-shifted by about 150 cm^{-1} for the one computed with the DFT surface. Also, the first small-intensity band, which has been assigned [8] to a (0,1) → (3,1) transition does not appear now in the spectrum obtained with the DFT surface. This is due to its higher dissociation energy, 3,719 cm^{-1}, for the DFT surface compared to the 3,449 cm^{-1} for the analytical TRIM-based one [8]. As we mentioned above, the (3,1) is now a bound level (see Fig. 3), while for the analytical surface this state is lying above the dissociation limit [8]. For the low temperature ($T = 1$ K) spectra of the D_5^+, we observed a similar behavior, with the main bands to be shifted to the higher frequencies, while again, the transitions to the red do not appear, due to the different dissociation energies of the PESs. In the top panels of Fig. 5, we indicate with arrows the energy positions of the present 2D theoretical threshold dissociation, estimates for both H_5^+ and D_5 using the DFT/B3(H) surface, as well as the reported ones for the analytical PES [8].

By comparing now the spectra obtained at $T = 300$ K, one can see that the features from the initial state at $T = 1$ K are conserved; however, new bands appear for higher energies due to the population of higher states according to the Boltzmann distribution. The transition energies, line intensities (see Eq. 7), and predissociation half-widths (see Eq. 8), for the main lines at $T = 300$ K, are listed in Table 1, together with the corresponding

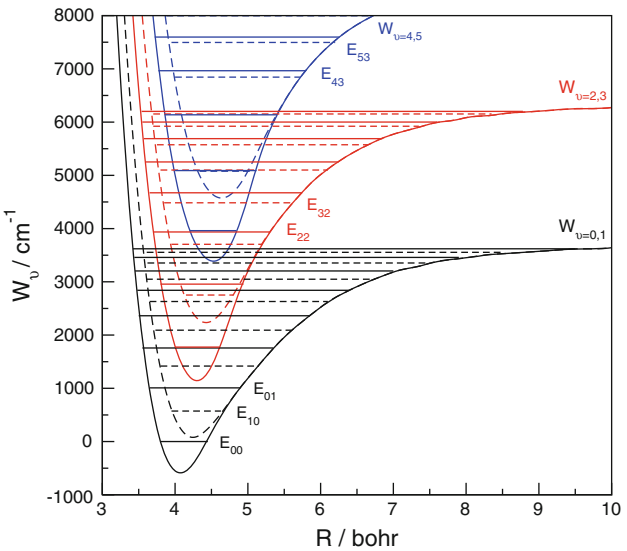

Fig. 3 Adiabatic effective $W_v(R)$ potential curves, and the corresponding E_{vn} energy levels for the H_5^+. *Solid lines* are for even $v = 0$, 2 and 4 values, while *dashed lines* for odd $v = 1$, 3 and 5 ones

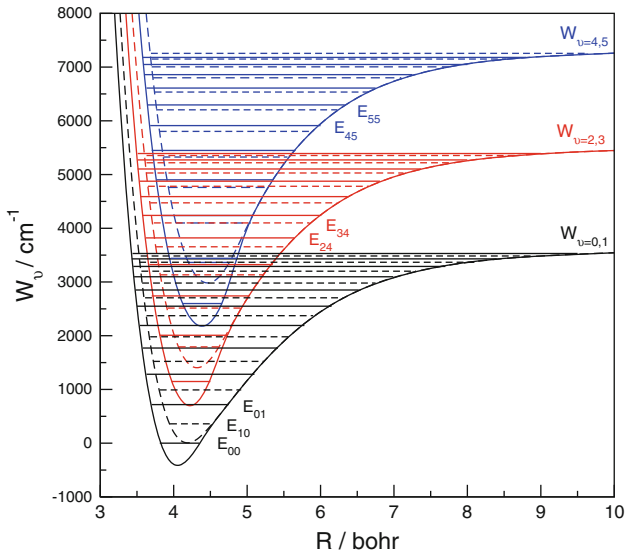

Fig. 4 Same as Fig. 3 for the D_5^+

assignment for each transition, for both H_5^+ and D_5^+ cations. The frequencies of the peaks assigned to the same transition in the spectrum obtained for H_5^+ and D_5^+ with the analytical and DFT surfaces are also shown in the bottom panels of Fig. 5.

In the inset plot of Fig. 5, we present comparison with the experimentally observed spectra. The calculated spectrum for the H_5^+ is in reasonable agreement, regarding the three main bands at 2,603, 3,520, and 4,232 cm^{-1}, assigned recently to excitation modes of the shared-proton mode [7]. The band at 3,904 cm^{-1} is missing from the both calculated spectra. We should note that this peak was previously assigned to the HH stretch [5, 7] and such motions are not taken into account in the present 2D model.

For the D_5^+ case, we can see that the calculated spectra are more congested than the H_5^+ ones; although the spectra from both surfaces present the same features, the one obtained with the DFT PES is shifted to higher frequencies. The comparison with the experiment shows the two main bands shifted to the red and with much lower intensity. Again the assignment to the features around 5,000 cm^{-1} corresponds to progression of the shared-proton mode (see Table 1). We should point out here that the agreement with the experiment for the D_5^+ looks worse than for H_5^+ for both PESs, and this is probably due to the higher anharmonicity of the D_5^+, as we can see in Fig. 4, indicating that the applied 2D model might not be very adequate in this case.

Finally, we should comment that the predissociation half-widths (see Table 1) for both surfaces are almost the same, and we found that are close to the experimental value estimated to 50 cm^{-1} [6]. On the other hand, we should also mention that the present estimates for the half-widths are larger by orders of magnitude than the ones from a previous theoretical calculation [31]. Predissociation half-widths strongly depend of the potential coupling between intra- and intermolecular modes and thus of the PES used. Moreover, in this latter study [31] the employed effective vibrational 3D model Hamiltonian includes only the HH stretching and intermolecular *R* modes, without taking into account the shared-proton mode [31]. Thus, such discrepancies should be attributed to the approaches, both for the potential and for the adiabatic kinetic energy operators,

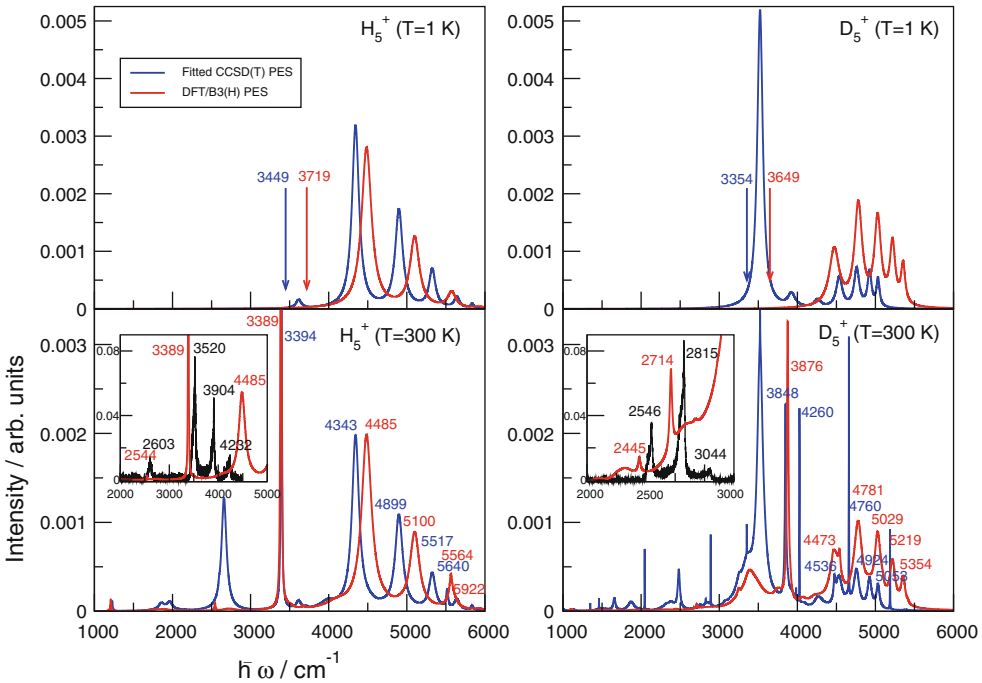

Fig. 5 IR calculated spectra at $T = 1$ K (*top panels*) and 300 K (*bottom panels*) for the H_5^+ (*left panels*) and D_5^+ (*right panels*) using the DFT/B3(H) surface [24] (*red lines*). The comparisons with previous simulations [8] employing the analytical surface [23] (*blue lines*) and with the experimental data [7] are also shown (*black lines* in the *inset plots*). The dissociation energy thresholds for the 2D systems are indicated with the corresponding arrows for each PES

Table 1 Assignments, frequency (in cm^{-1}), intensity (in a.u.), and predissociation half-widths (in cm^{-1}) for the main bands of the calculated IR spectra at $T = 300$ K of the H_5^+ and D_5^+ using the DFT/B3(H) surface

H_5^+				D_5^+			
$(v,n) \rightarrow (v',n')$	$\hbar\omega$	I	$\Gamma_{v'n'}$	$(v,n) \rightarrow (v',n')$	$\hbar\omega$	I	$\Gamma_{v'n'}$
(3,0) → (4,0)	1,209	3.8 (−1)	6	(3,2) → (4,2)	1,103	1.5 (−1)	12
(1,2) → (4,0)	1,870	1.5 (−4)	6	(3,3) → (4,3)	1,246	1.0 (−1)	13
(1,1) → (4,0)	2,544	4.3 (−4)	6	(3,1) → (4,2)	1,722	4.2 (−3)	12
(0,2) → (3,2)	2,727	5.0 (−3)	76	(3,0) → (4,2)	2,445	1.3 (−4)	12
(1,0) → (4,0)	3,389	9.3 (−4)	6	(1,2) → (4,2)	2,714	1.9 (−4)	12
(1,1) → (4,1)	3,673	3.7 (−4)	15	(1,1) → (4,2)	3,246	1.9 (−5)	12
(0,0) → (3,2)	4,485	1.4 (−4)	76	(0,1) → (3,4)	3,382	1.3 (−4)	79
(0,0) → (3,3)	5,100	5.9 (−5)	72	(0,1) → (3,5)	3,755	7.4 (−5)	75
(1,0) → (4,2)	5,564	5.1 (−5)	17	(1,0) → (4,2)	3,876	4.7 (−5)	12
(0,0) → (3,5)	5,922	7.7 (−7)	47	(0,1) → (3,6)	4,063	2.3 (−5)	58
				(1,1) → (4,4)	4,458	2.2 (−5)	13
				(0,0) → (3,5)	4,473	7.7 (−6)	75
				(1,0) → (4,3)	4,541	3.4 (−6)	13
				(0,0) → (3,6)	4,781	1.0 (−5)	58
				(0,0) → (3,7)	5,029	7.8 (−6)	50
				(0,0) → (3,8)	5,219	4.4 (−6)	41
				(0,0) → (3,9)	5,354	2.2 (−6)	31

Numbers in parenthesis are power of 10

adopted in each theoretical treatment. However, similar conclusions on the D_5^+ results have been also reported in this vibrational predissociation dynamics study of the H_5^+, using a completely different adiabatic approximation [31] than the present one.

4 Summary and conclusions

The IR photodissociation spectra of the H_5^+ and D_5^+ clusters are simulated by employing a two-dimensional adiabatic quantum model to describe the internal proton-transfer mode for these systems. Earlier and recent experiments using mass-selected photodissociation spectroscopy have been carried out, and several spectral bands have been observed and associated with excitations of the shared-proton mode. Given the importance of this motion to the assignment of IR photodissociation spectra for both H_5^+ and D_5^+ cations, we investigate here the effect of the underlying PES, employed in the theoretical simulations, on these spectral features. By comparing simulations with two completely different generated potential surfaces, namely TRIM/CCSD(T) fitted PES and DFT/B3(H) one, and analyzing the behavior of the emerged features in the spectra, we could evaluate the quality of the PESs and the influence of the errors in their generation to the dynamics of the systems under study. The analytical surface has been parameterized to high-level CCSD(T) data, and in general, it is expected to be more accurate than a DFT-based one. In one case, the source of errors is associated with the deviations obtained during the fitting procedure and the number and type of configurations of the computed ab initio data, while in the other one it has been shown that a realistic DFT-representation heavily relies on the choice of the functional.

With this in mind, we consider the comparison between the analytical and "on the fly" surfaces. As seen both of them reproduce quite similar theoretical spectra for both H_5^+ and D_5^+ clusters, with the peak positions, intensities and bandwidths of the obtained features being quantitatively comparable. Systematically, the bands calculated with the DFT surface for the H_5^+ appear shifted to higher frequencies by 150 cm^{-1}, and this is mainly attributed to the higher dissociation energy predicted by the DFT surface. We found that both theoretical spectra show a reasonable good agreement with the experimental spectrum of H_5^+ at $T = 300$ K. Both fitted surfaces for D_5^+ predict a more congested spectra than for the H_5^+ cluster. This is consistent with the deeper adiabatic effective, W_v, curves, producing very low intensities for the region between 1,500 and 3,500 cm^{-1} of the experimental bands. This indicates a possible limitation of the 2D adiabatic model for the heavier D_5^+ cluster. Regarding the potential surfaces, we may conclude that both of them could reproduce the main bands of the IR spectrum at energies between 3,000 and 6,000 cm^{-1} and associate them with excitations of the

shared-proton mode. The qualitative differences between them are mainly reflected only on the position of the peaks in the H_5^+, while in the spectra of the D_5^+ some variations are also found on the intensities.

Unfortunately, no more experimental results are yet available at the low-energy regime, where we should expect somehow larger quantitative differences between the two surfaces, and thus higher-dimensional models should be developed and employed to count with the highly fluxional nature of these cations. Work in this direction is in progress.

Acknowledgments This paper is dedicated to Prof. M. A. C. Nascimento on the occasion of his 65th birthday, with whom we had the opportunity to have several fruitful discussions. The authors would like to thank Prof. Duncan for providing his experimental results and the Centro de Calculo (IFF), CTI (CSIC), and CESGA for allocation of computer time. We would like also to thank Ricardo Pérez de Tudela for helpful discussions. This work has been supported by the Consolider-Ingenio 2010 Programme CSD2009-00038 (MICINN), the MICINN grant FIS2010-18132, and FIS2011-29596-C02-01, and COST Action CM1002 (CODECS). P. B. acknowledges a postdoctoral fellowship from the Spanish "Fundación Ramón Areces".

References

1. Dawson PH, Tickner AW (1962) J Chem Phys 37:672
2. Beuhler RJ, Ehrenson S, Friedman L (1983) J Chem Phys 79:5982
3. Hiraoka K (1987) J Chem Phys 87:4048
4. Hiraoka K, Mori T (1989) J Chem Phys 91:4821
5. Okumura M, Yeh LI, Lee YT (1998) J Chem Phys 88:79
6. Bae YK (1991) Chem Phys Lett 180:179
7. Cheng TC, Bandyopadyay B, Wang Y, Carter S, Braams BJ, Bowman JM, Duncan MA (2010) J Phys Chem Lett 1:758
8. Sanz-Sanz C, Roncero O, Valdés A, Prosmiti R, Delgado-Barrio G, Villarreal P, Barragán P, Aguado A (2011) Phys Rev A 84:060502-1–4
9. Acioli PH, Xie Z, Braams BJ, Bowman JM (2008) J Chem Phys 128:104318
10. Pérezde Tudela R, Barragán P, Prosmiti R, Villarreal P, Delgado-Barrio G (2011) J Phys Chem A 115:2483
11. Barragán P, Pérezde Tudela R, Prosmiti R, Villarreal P, Delgado-Barrio G (2011) Phys Scr 84:028109
12. Valdés A, Prosmiti R, Delgado-Barrio G (2012) J Chem Phys 136:104302
13. Yamaguchi Y, Gaw JF, Remington RB, Shaefer HF III (1987) J Chem Phys 86:5072
14. Farison M, Chermette H, Farizon-Mazuy B (1992) J Chem Phys 96:1325
15. Ignacio EW, Yamabe S (1998) Chem Phys Lett 287:563
16. Barbatti M, Jalbert G, Nascimento MAC (2000) J Chem Phys 113:4230
17. Müller H, Kutzelnigg W (2000) Phys Chem Chem Phys 2:2061
18. Prosmiti R, Buchachenko AA, Villarreal P, Delgado-Barrio G (2001) Theor Chem Acc 106:426
19. Moyano GE, Collins MA (2003) J Chem Phys 119:5510
20. Barbatti M, Nascimento MAC (2003) J Chem Phys 119:5444
21. Prosmiti R, Villarreal P, Delgado-Barrio G (2003) J Phys Chem A 107:4768
22. Xie Z, Braams BJ, Bowman JM (2005) J Chem Phys 122:224307
23. Aguado A, Barragán P, Prosmiti R, Delgado-Barrio G, Villarreal P, Roncero O (2010) J Chem Phys 133:024306
24. Barragán P, Prosmiti R, Roncero O, Aguado A, Villarreal P, Delgado-Barrio G (2010) J Chem Phys 133:054303
25. Roncero O, Beswick JA, Halberstadt N, Villarreal P, Delgado-Barrio G (1990) J Chem Phys 92:3348
26. López-Durán D, de Lara-Castells MP, Delgado-Barrio G, Villarreal P, di Paola C, Gianturco FA, Jellinek J (2004) Phys Rev Lett 93:053401
27. Aguado A, Sanz-Sanz C, Villarreal P, Roncero O (2012) Phys Rev A 85. Art ID 032514. doi:10.1103/PhysRevA.00.002500
28. Chermette H, Razafinjanahary H, Carrion L (1997) J Chem Phys 107:10643
29. Barragán P, Prosmiti R, Villarreal P, Delgado-Barrio G (2011) Int J Quantum Chem 111:368
30. Barragán P, Prosmiti R (2012) Int J Quantum Chem. doi:10.1002/qua.24026
31. Spirko V, Amano T, Kraemer WP (2006) J Chem Phys 124:244303